NANO LETTERS

2005
Vol. 5, No. 6
1123−1127

Femtosecond Imaging of Surface Plasmon Dynamics in a Nanostructured Silver Film

Atsushi Kubo,[†,§] Ken Onda,[†,§] Hrvoje Petek,*[,†,§] Zhijun Sun,[‡,§] Yun S. Jung,[‡,§] and Hong Koo Kim[‡,§]

Department of Physics and Astronomy, Department of Electrical Engineering, and Institute of NanoScience and Engineering, University of Pittsburgh, Pittsburgh, Pennsylvania 15260

Received April 10, 2005; Revised Manuscript Received May 6, 2005

ABSTRACT

Light interacting with nanostructured metals excites the collective charge density fluctuations known as surface plasmons (SP). Through excitation of the localized SP eigenmodes incident light is trapped on the nanometer spatial and femtosecond temporal scales and its field is enhanced. Here we demonstrate the imaging and quantum control of SP dynamics in a nanostructured silver film. By inducing and imaging the nonlinear two-photon photoemission from the sample with a pair of identical 10-fs laser pulses while scanning the pulse delay, we record a movie of SP fields at a rate of 330-attoseconds/frame.

Surface plasmon polaritons, or more simply, surface plasmons (SPs) are collective charge density fluctuations that can be excited by external optical fields at metal−vacuum or metal−dielectric interfaces.[1] The localization of electromagnetic fields through SP interference in nanometer scale metallic composites leads to the enhancement of nonlinear optical processes such as surface-enhanced Raman scattering (SERS),[2] second harmonic generation (SHG),[3,4] and multiphoton photoemission.[5−8] The coupling of light into SP modes occurs on nanostructured metals such as 1D and 2D metal gratings, metal nanoparticles, and rough metal films.[9−11] Recently, the prospect of plasmonic devices[12,13] has stimulated considerable effort to understand the fundamental dynamics of SPs[4−6,14,15] and to develop practical applications for sensing,[16] sub-wavelength optics,[17] waveguides,[12,18] circuits,[19] filters,[20] and interferometers.[21]

The physics of surface plasmons concerns the properties of electromagnetic fields on nanometer spatial and femtosecond temporal scales. The SP excitation makes possible subwavelength imaging with the near-field optical methods[11,22] and the propagation of light through subwavelength apertures.[23] The T_2 dephasing times on femtosecond time scales determine the lengths of propagation and coherent interaction of SP modes.[4,5,14,24] The subwavelength spatial and femtosecond temporal coherence properties impose severe experimental requirements for the investigation of SP dynamics. To date, sub-wavelength spatial imaging has been achieved by scanning near-field optical microscopy (SNOM),[10,12,22,25,26] and femtosecond time resolution has been realized by interferometric two-pulse correlation techniques.[4,5,14,15] However, the simultaneous imaging of SP modes on their fundamental spatial and temporal scales has not been possible by optical methods.[26]

Here we demonstrate a new technique for investigating surface plasmon dynamics with sub-femtosecond temporal precision and sub-wavelength spatial resolution. We combine the techniques of interferometric time-resolved two-photon photoemission (ITR-2PP)[27−29] and photoelectron emission microscopy (PEEM).[8,30] Phase correlated pump and probe optical pulses with 10 fs duration excite SP modes in a silver film with nanoscale periodic and random topography. Imaging of electrons with the PEEM electron optics creates a map of SP fields that mediate two-photon photoemission. ITR-2PP is a powerful method to extract the dynamical information about the dephasing of collective[31] as well as single-particle excitations in metals and at their surfaces.[29] Imaging electrons with a PEEM makes possible the imaging of SPs modes with spatial resolution beyond the limits of conventional far-field optics.[8] The possibility of high spatio-temporal resolution imaging through a combination of ultrafast laser and electron optic methods has been demonstrated before, though no actual time-resolved measurements have been performed.[32,33] In this letter we present a movie of the spatio-temporal evolution of SP fields with a 50-nm spatial resolution taken at with 330-as/frame (see Supporting

* Corresponding author. E-mail: petek@pitt.edu
† Department of Physics and Astronomy.
‡ Department of Electrical Engineering.
§ Institute of NanoScience and Engineering.

10.1021/nl0506655 CCC: $30.25
Published on Web 05/17/2005

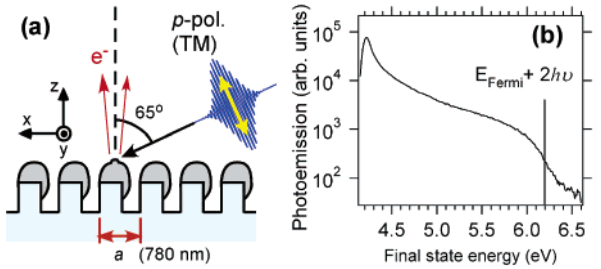

Figure 1. (a) Schematic structure of the silver grating sample and excitation conditions with the 10 fs laser pulses. The silver grating is formed by angled evaporation of silver onto a patterned quartz substrate. (b) Two-photon photoemission spectrum of the silver grating sample excited with the 400-nm (3.1 eV) femtosecond pulses.

Information). This unprecedented temporal resolution is achieved by scanning the delay between 10 fs duration pump−probe pulse with 50-as temporal precision. We demonstrate the coherent control of plasmonic fields[28,34−36] through the phase of the excitation light, which allows us to specify the creation and annihilation of the localized SP fields at a specific point in space and time.

Figure 1a shows a schematic of the excitation process of SP modes in a nanostructured sample by a femtosecond laser pulse. The excitation light is the second harmonic of a self-made Ti:sapphire laser oscillator, providing 10 fs pulses at 400 nm center wavelength with 100 mW average power and 90 MHz repetition frequency. The excitation light is compensated for the optical dispersion to achieve the minimum pulse duration at the sample.[29] The incident light at 65° from the surface normal irradiates a 180 × 120-μm diameter spot at the focal plane of the PEEM (FOCUS GmbH). Photoemission is induced by two photons from the laser ($h\nu$ = 3.10 eV) or single photons from a conventional Hg lamp ($h\nu$ = 4.89 eV), both of which can excite electrons above the work function of the sample (4.2 eV).

The sample is a silver grating, which has the properties of an optical band-pass transmission filter. Details of the sample fabrication and its optical properties are reported in ref 20. The silver photonic structure is formed by angled deposition onto a one-dimensional array of mesa structures photolithographically formed on a quartz substrate (Figure 1a). The resulting 400 nm thick silver film is perforated by an array of 100 nm wide slits with a period of 780 nm. A scanning electron microscope (SEM) image in the Figure 2a inset shows the topography of the grating including random <10 nm scale surface roughness of the silver film. These periodic and random structures couple the external optical field into the propagating and localized SP modes of the sample.

Figure 1b shows a two-photon photoemission (2PP) spectrum of the sample taken by a hemispherical electron energy analyzer for excitation with the p-polarized (TM) 400-nm laser light. The spectrum shows simple structure; the maximum emission intensity occurs at the vacuum edge, and the signal decreases monotonically to the Fermi level edge. Such spectra are characteristic for plasmon-mediated two-photon photoemission from silver nanoparticles,[5] where the kinetic energy of photoelectrons represents the distribution of hot electrons generated by the decay of multiply excited plasmons. The spectrum is distinctly different from that of single crystalline silver samples, which are dominated by band-to-band single particle (electron−hole pair) excitations.[37]

The coupling of light into the propagating surface plasmon modes of the photonic grating structure at the silver−vacuum interface is possible at an incident angle of $\theta = 38°$ from the surface normal. The resonant condition given by $(\omega/c)\sin\theta + 2\pi/a = (\omega/c)[\epsilon/(1+\epsilon)]^{1/2}$, where ω is the angular frequency of light, a the grating period, and ϵ the real part of the dielectric function of silver ($\epsilon \approx -4.4$ at 400 nm), is derived by matching of phase velocity of light with that of the SP modes of silver within an integer reciprocal vector of the grating. The resonant condition is confirmed separately by angle-resolved photoemission spectroscopy; the PEEM sample holder, however, allows excitation only at $\theta = 65°$. At this angle the excitation of propagating modes is suppressed and mainly the localized SP modes are excited.

One- and two-photon photoemission (1PP-PEEM and 2PP-PEEM) images of the same part of the sample in Figure 2 are excited with the unpolarized Hg lamp (a), the p-polarized (TM) laser (b), and the s-polarized (TE) laser (c). The 1PP-PEEM and SEM images both show topography of the sample, except for the film roughness, which is too fine to resolve with the PEEM. Because the 4.89-eV light is above the plasmon resonances of silver,[7] the 1PP-PEEM image maps the probability of exciting single-particle excitations in the bulk silver, which is uniform for the polycrystalline silver sample.

By contrast, the 2PP-PEEM image in Figure 2b shows considerably richer structure, being punctuated by intense "hot spots",[8] which are ~20 times stronger than the emission from the underlying grating lines. In addition, both intensities and distribution of hot spots depend sensitively on polarization. For example, intensities of dots framed by the rectangle in Figure 2b are enhanced for p-polarized light by more than two orders of magnitude compared with the emission excited with s-polarized light. We attribute the differences with respect to the 1PP-PEEM image and the strong polarization dependence for the 2PP-PEEM images to excitation of the surface plasmon fields on the nanometer scale. Such enhancement effects have been predicted by theory and observed by near-field microscopy in disordered nanostructured metal films.[10,38,39]

The resonance frequencies of SP eigenmodes extend from the eigenenergy of the bulk plasmon of Ag at 3.8 eV to infrared depending on the local structure, interparticle coupling, and particle shape. The usual approach to modeling of the optical properties of rough metal surfaces is to approximate the film morphology by metal spheroids. For small Ag particles supported on insulator and semiconductor substrates, local minima in the reflection and peaks in the 2PP yield spectra at ~3.3 and ~3.7 eV and have been attributed to the excitation surface plasmon eigenmodes of metal spheroids (Mie Plasmons).[7,8,40] As the metal spheroids percolate and coalesce into irregularly shaped cluster com-

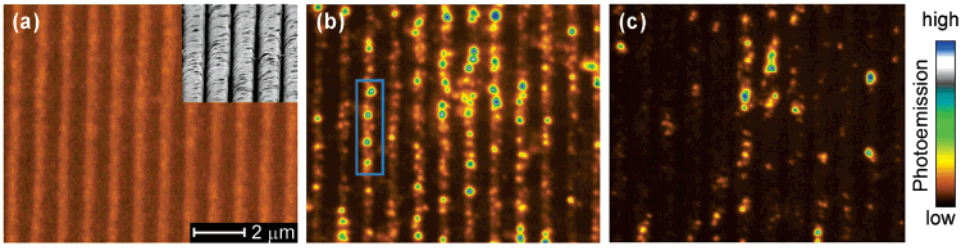

Figure 2. (a−c) PEEM micrographs of the identical region on the silver grating obtained with (a) 254-nm line of a Hg lamp (1PP-PEEM), (b) p-polarized 400-nm femtosecond laser excitation (2PP-PEEM), and (c) s-polarized 400-nm femtosecond laser excitation (2PP−PEEM). Image contrast of (c) is enhanced by three times compared with (b). The scanning electron micrograph (SEM) of the silver grating in (a) is superimposed with the 1PP-PEEM image to show correspondence in the >100 nm scale topographical contrast. The surface roughness with <10 nm RMS distribution in the SEM image, which is too fine to resolve with the PEEM, gives rise to excitation of the localized SP modes seen as the hot spots in the 2PP-PEEM images of (b) and (c). The blue rectangle locates the four hot spots featured in Figure 3.

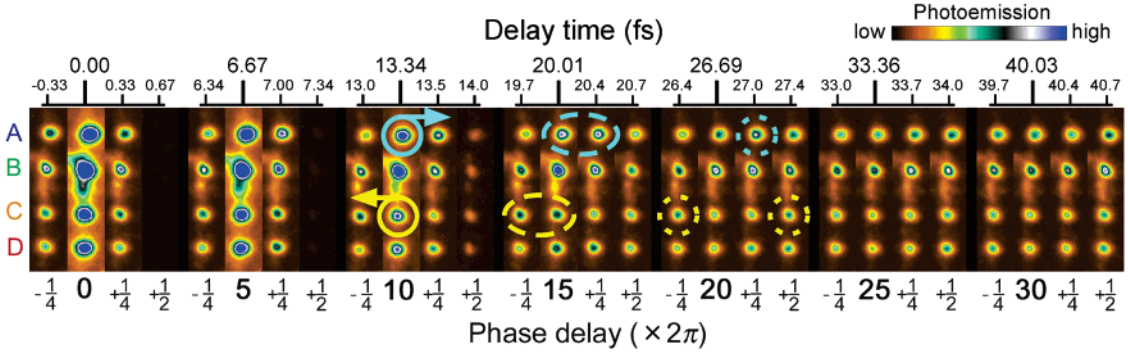

Figure 3. Interferometric time-resolved photoelectron emission micrographs (ITR-PEEM) of the four localized plasmons on the silver grating framed in Figure 2b. The delay time between the pump and probe pulses (τ_d) is advanced from −0.33 fs to 40.69 fs or $-^1/_4 \times 2\pi \rightarrow 30^1/_2 \times 2\pi$ in terms of the optical phase of the carrier light ($\lambda = 400$ nm) with an increment step of 0.33 fs or $1/2\pi$. All four dots oscillate in-phase with the field during the optical excitation by the pump pulse ($-^1/_4 \times 2\pi \rightarrow 5^1/_2 \times 2\pi$). As the driving pulse wanes, the coherent polarization excited at each dot shifts to its own resonant frequency. For instance, the phase of dots A, B, and D (dot C) is retarded (advanced), causing the intensity maxima to rise later (sooner) with respect to the phase of the driving field. The circled hotspots indicate the change in the intensity maxima (constructive interference) in five cycle intervals due to the phase slip of the SP modes with respect to the driving field.

posites, the distribution of the SP modes broadens and extends to IR frequencies. Theoretical simulations of such semicontinuous metal films show that local SP mode resonances spread from the visible to infrared frequencies and fields are strongly enhanced due to the localization of light.[10,39] For effectively continuous films, such as investigated here, the SP modes can be excited at metallic voids, protrusions, and other regions of nanoscale roughness. The intensity of 2PP excited with p-polarized light is probably due to the surface photoelectric effect; that is, the field enhancement associated with the excitation of longitudinal surface fields below the bulk plasmon resonance of silver.[41] The 'hot spot' structures in Figure 2b,c thus represent a nonlinear map (2PP emission has an E^4 dependence on the electric field of the excitation light) of local SP fields excited in the sample. The density of hot spots in the 2PP-PEEM images of the grating is considerably less than the density of protrusions visible in the SEM image, because the 400 nm laser is resonant with only a fraction of SP resonances in granular Ag films.[10,40,42] Moreover, the spatial resolution of the PEEM is insufficient to resolve the characteristic structures of individual hot spots. The grating structure may also couple the laser field into the propagating SP modes, as introduced above, but for the specific choice of excitation geometry and grating period the excitation of such modes is suppressed.

Because surface plasmons are coherent electromagnetic excitations that undergo spatio-temporal phase evolution in nanometer scale metallic structures, we further investigate their coherent dynamics[28] by recording interferometric time-resolved PEEM (ITR-PEEM) movies. For these measurements, the 10 fs excitation laser pulses are split into identical collinear replicas by transmission through a Mach−Zender interferometer (MZI). Interferometric scanning of the length of one arm of the MZI modulates their mutual delay τ_d with better than 50 as accuracy, corresponding to <1/25 of an optical cycle (1.33 fs) of the 400-nm light.[29] By advancing the delay in 1/4-cycle steps, we record a movie of the SP dynamics with an interval of 330 as/frame (see Supporting Information).

We focus our study of the coherent dynamics on the four intense SP modes highlighted in Figure 2b, which we investigate by two complementary methods. Figure 3 presents select frames of an ITR-PEEM movie where we extract the portion of each image showing the four hot spots. We record the movie by advancing the delay from $\tau_d = -0.33$ fs to 40.69 fs in steps of 0.33 fs, or in terms of the phase of the carrier wave, from $\phi = -^1/_4 \times 2\pi$ to $30^1/_2 \times 2\pi$ in steps of

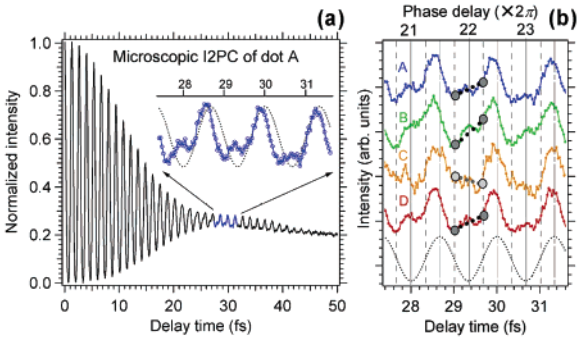

Figure 4. Microscopic interferometric two-pulse correlation (I2PC) scans from individual hot spots. (a) I2PC from dot A (Figure 3). The inset magnifies a portion of the scan for the delay of 27.4−31.6 fs. (b) Comparison of the I2PC wings for dots A−D in the same time interval as the inset of (a). Each hot spot shows mode-specific beating pattern after the pump pulse has passed reflecting the individual resonance frequency and dephasing time. For instance, the signal intensity of dot C decreases for the phase delay of $21^3/_4 \times 2\pi \rightarrow 22^1/_4 \times 2\pi$, while others increase (dashed lines), consistent with the higher frequency of C. The optical interference of the 400 nm carrier wave (dotted lines in (a) and (b)) serves as a 1.33 fs period clock for timing the evolution of the SP polarization waves.[27]

$\pi/2$. Alternatively, quantitative phase evolution of each mode is recorded in interferometric two-pulse correlation (I2PC) scans, where we measure the intensity of each hot spot while continuously scanning τ_d (Figure 4).

The movie frames in Figure 3 and I2PC scans in Figure 4 follow the temporal evolution of the coherent polarization excited in each dot. When τ_d is short compared with the pulse duration, the excitation field drives the coherent plasmon oscillations;[4] the modulation of images and fringes is dominated by the interference between the pump and probe optical fields at the carrier frequency. On the intermediate time scales ($5 \times 2\pi \geq \tau_d \geq 30 \times 2\pi$) when the pump and probe pulses no longer overlap, the memory of the phase of the pump pulse is still retained in the coherent plasmon fields, and the interference occurs between the pump and probe induced polarization waves excited in the sample. However, now each dot oscillates at its characteristic resonance frequency. The polarization waves dephase through coupling with other SP modes or by decaying into single-particle excitations.[4,6] On the longest time scales ($\tau_d \geq 30 \times 2\pi$), the coherent polarization has dephased and polarization waves no longer interfere. However, there remains an exponentially decaying signal from hot electrons, which are generated by the SP decay.[6] We fit the I2PC scans according to the model of Lehmann et al. for the SP-enhanced 2PP from Ag nanoparticles,[5] and hot-electron decay in metals.[29] Fitting the I2PCs for dots A−D gives a range of dephasing times $T_2 = 4.9-5.8$ fs, which are comparable to those from the previous line width and second harmonic measurements for silver nanoparticles.[4,24] We note that similar attosecond field fluctuations have been predicted by Stockman et al. to occur in percolated silver films.[39]

The interference patterns at the intermediate delays in Figure 4b provide further information on the mode-specific coherent polarization dynamics. The phase of each mode evolves according to its resonance frequency. The mode specificity can be seen in Figure 4b, where advancing the phase by π from $21^3/_4 \times 2\pi$ causes the intensity of dot C to decrease while that of others increases. This trend is consistent with the images in Figure 3, where the phase of dot C is advanced, while the phases of the other dots are retarded with respect to the driving frequency, as indicated by yellow and blue highlights for C and A. These phase-dependent intensities indicate that the resonance frequency of C is higher than the optical carrier frequency, and hence it evolves faster, while those of the other dots are lower, and hence they evolve more slowly. Significantly, the higher frequencies correlate with the faster T_2 dephasing times as expected from the imaginary part of the dielectric constant of silver.[1]

We can understand the SP oscillations in Figures 3 and 4 in terms of quantum interference between pump- and probe-induced polarization waves.[27,28] The 10 fs laser pulses excite a distribution of SP modes with resonant frequencies that fall within their 27 nm bandwidth. The pump pulse drives the collective electron oscillations at the optical carrier frequency, but after the pulse passes, the individual modes evolve according to their natural frequencies and couplings with the dephasing and dissipative degrees of freedom. The phases evolve into or out of phase with the probe field at specific delay times, leading to the constructive or destructive interferences, which are observed as the enhanced or suppressed photoemission.[28] Considering the interference in the frequency domain, the spectrum of a pulse-pair for $\tau_d \neq 0$ is narrower and more structured than the spectrum of individual pulses: Some frequency components of the pulse pair interfere constructively while others interfere destructively when recorded with a spectrometer, or as an outcome of interaction with material excitations possessing coherence times that are comparable to or longer than the pulse.[34] In atomic physics, this sinusoidal modulation of the spectrum with the relative phase of the pulse pair is known as the optical Ramsey fringe effect.[43] If an SP resonance coincides with a Ramsey fringe minimum, it is excited for times less than τ_d, but on arrival of the probe pulse, the localized plasmon field created by the pump adds coherently to the reflected propagating field of the probe, leaving the SP resonance unexcited.[27,28] Based on this model, we can understand the characteristic intensity fluctuations of the dots in Figure 3: As the delay is advanced by π from $14^3/_4 \times 2\pi$, the spectral maximum of the pulse-pair excitation field shifts from 396 to 407 nm. Considering this red shift and intensities in Figure 3, we conclude again that the resonance wavelengths of dots A, B, and D are longer than 400 nm, while that of dot C is shorter.

The localization of plasmon fields in individual dots at specific pump−probe delays in Figure 3 constitutes a realization of quantum control.[28,34−36] By selecting excitation fields through a choice of τ_d, we specify the excitation and deexcitation of individual plasmon resonances with <50 as temporal and <50 nm spatial accuracy. With more complex methods, it is now possible to engineer control fields with arbitrary spatial and temporal phase that are limited only by

bandwidths of the existing ultrafast laser sources.[44] By using thus engineered optical fields, we can control the spatio-temporal evolution of plasmon fields and other coherent excitations within systems of metallic and semiconductor nanostructures. The ability to image the time-evolution of SP fields by the ITR-PEEM technique opens the way to study the dynamical properties of nanophotonic devices.[13] Theoretical schemes for the quantum control of energy localization and stimulated plasmon amplification have already been proposed by Stockman and co-workers.[45,46] The present imaging and control fields are not only applicable to localized SP fields, as demonstrated here, but also to propagating modes of plasmonic nanostructures as well as atomically smooth metallic films.

In summary, by combining the ultrafast laser spectroscopy and electron microscopy we image the quantum interference of localized SP polarization waves with subwavelength spatial resolution and subfemtosecond temporal precision. This development advances the time-resolution of electron microscopy for imaging the fundamental excitations in solids by more than twelve orders of magnitude. The dynamical imaging of surface plasmons in the suboptical cycle regime adds a new dimension to the study of plasmonic nanostructures.

Acknowledgment. The authors thank H.-J. Freund, W. Drachsel, and W. Benten for the opportunity to join some early TR-PEEM experiments and A. P. Heberle for illuminating discussions. This research has been supported by NSF DMR-0116034 and NSF ECS-0403865 grants. A. K. acknowledges fellowship support from Yamada Science Foundation of Japan.

Supporting Information Available: ITR-PEEM movies of Figure 2b and Figure 3 as .avi files. This material is available free of charge via the Internet at http://pubs.acs.org.

References

(1) *Surface Plasmons*; Raether, H., Ed.; Springer: Berlin, 1988.
(2) Kneipp, K.; Wang, Y.; Kneipp, H.; Perelman, L. T.; Itzkan, I.; Dasari, R. R.; Feld, M. S. *Phys. Rev. Lett.* **1997**, *78*, 1667.
(3) Chen, C. K.; de Castro, A. R. B.; Shen, Y. R. *Phys. Rev. Lett.* **1981**, *46*, 145.
(4) Lamprecht, B.; Leitner, A.; Aussenegg, R. R. *Appl. Phys. B* **1999**, *68*, 419.
(5) Lehmann, J.; Merschdorf, M.; Pfeiffer, W.; Thon, A.; Voll, S.; Gerber, G. *Phys. Rev. Lett.* **2000**, *85*, 2921.
(6) Merschdorf, M.; Pfeiffer, W.; Thon, A.; Voll, S.; Gerber, G. *Appl. Phys. A* **2000**, *71*, 547.
(7) Monchicourt, P.; Raynaud, M.; Saringar, H.; Kupersztych, J. *J. Phys. Condens. Matter* **1997**, *9*, 5765.
(8) Fecher, G. H.; Schmidt, O.; Hwu, Y.; Schönhense, G. *J. Electron Spectrosc. Relat. Phenom.* **2002**, *126*, 77.
(9) García-Vidal, F. J.; Martín-Moreno, L. *Phys. Rev. B* **2002**, *66*, 155412.
(10) Sarychev, A. K.; Shalaev, V. M. *Phys. Rep.* **2000**, *335*, 275.
(11) Barber, P. W.; Chang, P. K.; Massoudi, H. *Phys. Rev. Lett.* **1983**, *50*, 997.
(12) Barnes, W. L.; Dereux, A.; Ebbesen, T. W. *Nature* **2003**, *424*, 824.
(13) Van Duyne, R. P. *Science* **2004**, *306*, 985.
(14) Lamprecht, B.; Krenn, J. R.; Leitner, A.; Aussenegg, F. R. *Phys. Rev. Lett.* **1999**, *83*, 4421.
(15) Zentgraf, T.; Christ, A.; Kuhl, J.; Giessen, H. *Phys. Rev. Lett.* **2004**, *93*, 243901.
(16) McFarland, A. D.; van Duyne, R. P. *Nano Lett.* **2003**, *3*, 1057.
(17) Devaux, E.; Ebbesen, T. W.; Weeber, J.-C.; Dereux, A. *Appl. Phys. Lett.* **2003**, *83*, 4936.
(18) Krenn, J. R.; Salerno, M.; Felidj, N.; Lamprecht, B.; Schider, G.; Leitner, A.; Aussenegg, F. R.; Weeber, J. C.; Dereux, A.; Goudonnet, J. P. *J. Microscopy* **2001**, *202*, 122.
(19) Maier, S. A.; Brongersma, M. L.; Kik, P. G.; Atwater, H. A. *Phys. Rev. B* **2002**, *65*, 193408.
(20) Sun, Z.; Jung, Y. S.; Kim, H. K. *Appl. Phys. Lett.* **2003**, *83*, 3021.
(21) Ditlbacher, H.; Krenn, J. R.; Schider, G.; Leitner, A.; Aussenegg, F. R. *Appl. Phys. Lett.* **2002**, *81*, 1762.
(22) Hartschuh, A.; Beversluis, M. R.; Bouhelier, A.; Novotny, L. *Philos. Trans. R. Soc. London A* **2004**, *362*, 807.
(23) Ebbesen, T. W.; Lezec, H. J.; Ghaemi, H. F.; Thio, T.; Wolff, P. A. *Nature* **1998**, *391*, 667.
(24) Nilius, N.; Ernst, N.; Freund, H.-J. *Phys. Rev. Lett.* **2000**, *84*, 3994.
(25) Hecht, B.; Bielefeldt, H.; Novotny, L.; Inouye, Y.; Pohl, D. W. *Phys. Rev. Lett.* **1996**, *77*, 1889.
(26) Imura, K.; Nagahama, T.; Okamoto, H. *J. Phys. Chem. B* **2004**, *108*, 16344.
(27) Ogawa, S.; Nagano, H.; Petek, H.; Heberle, A. P. *Phys. Rev. Lett.* **1997**, *78*, 1339.
(28) Petek, H.; Heberle, A. P.; Nessler, W.; Nagano, H.; Kubota, S.; Matsunami, S.; Moriya, N.; Ogawa, S. *Phys. Rev. Lett*. **1997**, *79*, 4649.
(29) Petek, H.; Ogawa, S. *Prog. Surf. Sci.* **1997**, *56*, 239.
(30) Rotermund, H. H. *Surf. Sci. Rep.* **1997**, *29*, 265.
(31) Merschdorf, M.; Kennerknecht, C.; Pfeiffer, W. *Phys. Rev. B* **2004**, *70*, 193401.
(32) Schmidt, O.; Bauer, M.; Wiemann, C.; Porath, R.; Scharte, M.; Andreyev, O.; Schönhense, G.; Aeschlimann, M. *Appl. Phys. B* **2002**, *74*, 223.
(33) Sekatskii, S. K.; Chekalin, S. V.; Ivanov, A. L.; Matveets, Y. A.; Stepanov, A. G.; Letokhov, V. S. *J. Phys. Chem. A* **1998**, *102*, 4148.
(34) Heberle, A. P.; Baumberg, J. J.; Köhler, K. *Phys. Rev. Lett.* **1995**, *75*, 2598.
(35) Shapiro, M.; Brumer, P. *Rep. Prog. Phys.* **2003**, *66*, 859.
(36) Warren, W. S.; Rabitz, H.; Dahleh, M. *Science* **1993**, *259*, 1581.
(37) Pontius, N.; Sametoglu, V.; Petek, H.; Eberhardt, W. *Phys. Rev. B*, submitted.
(38) Gresillon, S.; Aigouy, L.; Boccara, A. C.; Rivoal, J. C.; Quelin, X.; Desmarest, C.; Gadenne, P.; Shubin, V. A.; Sarychev, A. K.; Shalaev, V. M. *Phys. Rev. Lett.* **1999**, *82*, 4520.
(39) Stockman, M. I. *Phys. Rev. B* **2000**, *62*, 10494.
(40) Yoshida, S.; Yamaguchi, T.; Kinbara, A. *J. Opt. Soc. Am.* **1972**, *62*, 1415.
(41) Levinson, H. J.; Plummer, E. W. *Phys. Rev. B* **1981**, *24*, 628.
(42) Stockman, M. I.; Pandey, L. N.; George, T. F. *Phys. Rev. B* **1996**, *53*, 2183.
(43) Salour, M. M.; Cohen-Tannoudji, C. *Phys. Rev. Lett.* **1977**, *38*, 757.
(44) Feurer, T.; Vaughan, J. C.; Nelson, K. A. *Science* **2003**, *299*, 374.
(45) Stockman, M. I.; Faleev, S. V.; Bergman, D. J. *Phys. Rev. Lett.* **2002**, *88*, 067402.
(46) Bergman, D. J.; Stockman, M. I. *Phys. Rev. Lett.* **2003**, *90*, 027402.

NL0506655